

Wavelength selective coupler with vertical gratings on silicon chip

Kazuhiro Ikeda,^{a)} Maziar Nezhad, and Yeshaiahu Fainman
 Department of Electrical and Computer Engineering, University of California, San Diego, 9500 Gilman Drive, La Jolla, California 92093-0409, USA

(Received 29 February 2008; accepted 5 May 2008; published online 23 May 2008)

We propose a wavelength selective coupler using vertical grating structure on silicon chip and discuss the operation principle and the analytic design procedure. The transmission spectra expected by the procedure agree with finite difference time domain simulation results. We then fabricate the designed wavelength selective coupler and demonstrate the expected operation. The available wavelength-division-multiplexing bandwidth of this device is not limited by free spectral range as in ring resonators. We also propose some applications of the wavelength selective coupler. © 2008 American Institute of Physics. [DOI: 10.1063/1.2936862]

Silicon-based functional optical devices compatible with a standard complementary metal-oxide semiconductor technology, such as modulator, filter, and detector, are desirable for the realization of on-chip optical interconnections with high capacity.¹ The development of compact devices using a single lithographic step is essential for cost-effective manufacturing with the standard silicon technology. To meet this objective, we recently constructed a compact silicon photonic device using vertical grating (VG) structure^{2,3} although a similar grating structure but with different waveguide geometry had been reported in Ref. 4. The sidewalls of a channel-type waveguide are modulated (we call this structure VG) to impose a Bragg condition for the propagating waveguide modes. This structure can be simply integrated upon the definition of the waveguide geometry without additional lithographic process, while horizontal gratings require an additional process after fabricating the waveguide. This VG structure is useful for filters, resonators, and modulators, as demonstrated in Ref. 3. In this letter, we report a pair of coupled VG waveguides that create a wavelength selective coupler (WSC) to implement a compact add-drop device useful for wavelength division multiplexing (WDM). We describe the design, fabrication, and characterization of our add-drop device. Our device has very large free spectral range (FSR), supporting the total bandwidth of about 70 nm used in WDM systems, whereas the FSR of a ring resonator implementation is limited to about 20 nm for typical ring designs with radius of about 5 μm.¹

Figure 1(a) shows the schematic diagram of WSC that we discuss in this letter. Two waveguides WG1 and WG2 with VGs are placed close together with a gap (G), which have different widths (W₁ and W₂) and grating depths (ΔW₁ and ΔW₂) but same grating periods (Λ). In this structure, we have three Bragg conditions as follows:⁵

$$2\beta_1 = \frac{2\pi}{\Lambda}, \tag{1a}$$

$$2\beta_2 = \frac{2\pi}{\Lambda}, \tag{1b}$$

$$\beta_1 + \beta_2 = \frac{2\pi}{\Lambda}, \tag{1c}$$

where β₁ and β₂ are the propagation constants for WG1 and WG2, respectively. Equations (1a)–(1c) represent the backward coupling in WG1, the backward coupling in WG2, and the cross coupling between WG1 and WG2, respectively. We perform the following process to design the device: (a) Allocate the three Bragg conditions to desired wavelengths by choosing W₁, W₂, and Λ. (b) Determine the coupling coefficients to achieve the desired bandwidths for the Bragg conditions using ΔW₁, ΔW₂, and G. (c) Determine the length of

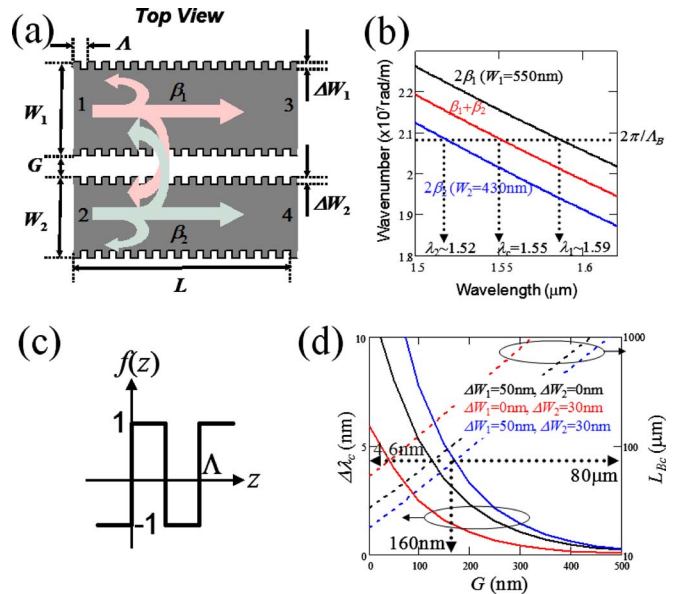


FIG. 1. (Color online) (a) Schematic diagram of the WSC with VG structure. (b) Propagation constants calculated for TE polarization by 2D analysis with effective index method, assuming that the thickness of the silicon slab is 250 nm and the silicon slab is sandwiched by silica claddings. The solid lines are the plots of the left-hand sides of the Bragg conditions, Eqs. (1a)–(1c). The dotted horizontal line indicates the wavenumber of the grating, i.e., the right-hand sides of Eqs. (1a)–(1c). The cross points of the solid lines and the dotted line are the three Bragg conditions: (c) Periodic function $f(z)$ used for calculating the coupling coefficients, (d) plots of the bandwidth $\Delta\lambda_c$, and Bragg length L_{bc} for cross coupling with relation to the gap G , for several grating depths, $\Delta W_1=50$ nm and $\Delta W_2=0$ nm, $\Delta W_1=0$ nm and $\Delta W_2=30$ nm, and $\Delta W_1=50$ nm and $\Delta W_2=30$ nm.

^{a)}Electronic mail: kaziked@ucsd.edu.

the structure to obtain the desired extinctions. These steps are further described below.

We begin with allocating the Bragg conditions as follows: At the first step, we pick up some reasonable values of W_1 and W_2 , assuming that the thickness of the silicon core is 250 nm and the silicon core is surrounded by silica cladding. In this specific example, we take $W_1=550$ nm and $W_2=430$ nm, and calculate β for TE polarization by two-dimensional (2D) analysis with effective index method. (The effect of the grating on the propagation constants is neglected.) The solid lines in Fig. 1(b) are the plots of the left-hand sides of the Bragg conditions [Eqs. (1a)–(1c)]. The dotted horizontal line in Fig. 1(b) indicates the wavenumber of the grating, i.e., the right-hand sides of Eqs. (1a)–(1c). Therefore, the cross points of the solid and the dotted lines provide the three Bragg conditions. We now calculate Λ_B to set a specific wavelength at cross coupling ($\lambda_c=1.55$ μm for this example) using Eq. (1c) as, $\Lambda_B=2\pi/\{\beta_1(\lambda=1.55$ $\mu\text{m})+\beta_2(\lambda=1.55$ $\mu\text{m})\}=301$ nm. With this value of Λ_B , we find the corresponding wavelengths, λ_1 and λ_2 for the other Bragg conditions of Eqs. (1a) and (1b), and check if these are at the desired wavelengths. In our design example, we tried to allocate these backward couplings outside the C band and indeed these wavelengths locate outside C band with this design ($\lambda_1\sim 1.52$ μm and $\lambda_2\sim 1.59$ μm). Note that these stopbands may be also used for bandstop filters together with the cross coupling. If the designed Bragg wavelengths are not appropriate, then we repeat the above procedure until the desired Bragg conditions are satisfied.

Next, we determine the coupling coefficients and the length of the device. The coupling coefficients are given by the following formulas using coupled mode theory,^{5,6}

$$\kappa_1 = \frac{\varepsilon_0\omega}{4}\langle E_1|\Delta n_g^2|E_1\rangle, \quad (2a)$$

$$\kappa_2 = \frac{\varepsilon_0\omega}{4}\langle E_2|\Delta n_g^2|E_2\rangle, \quad (2b)$$

$$\kappa_c = \frac{\varepsilon_0\omega}{4}\langle E_1|\Delta n_g^2|E_2\rangle, \quad (2c)$$

with

$$\Delta n_g^2 = \begin{cases} -(n_{\text{core}}^2 - n_{\text{clad}}^2)\frac{f(z)+1}{2} & \text{in grating region} \\ 0 & \text{otherwise,} \end{cases} \quad (2d)$$

where κ_1 , κ_2 , and κ_c are the coupling coefficients for the backward coupling in WG1, the backward coupling in WG2, and the cross coupling between WG1 and WG2, respectively, ε_0 is the vacuum permittivity, ω is the angular frequency of light, E_1 and E_2 are the field distributions in WG1 and WG2, which are calculated for TE polarization again using 2D effective index method, Δn_g indicates the index perturbation which has values only at the grating region, n_{core} and n_{clad} are the silicon core effective index 2.96 and the silica cladding refractive index 1.4, and $f(z)$ is a periodic function shown in Fig. 1(c), where z is the coordinate along the grating waveguide. Intuitively, the larger the modulation (i.e., larger ΔW_1 and ΔW_2) and the field overlap (i.e., smaller W_1 , W_2 , and G), the larger the coupling coefficients. For known coupling coefficients, we can estimate the coupling bandwidths $\Delta\lambda_i$

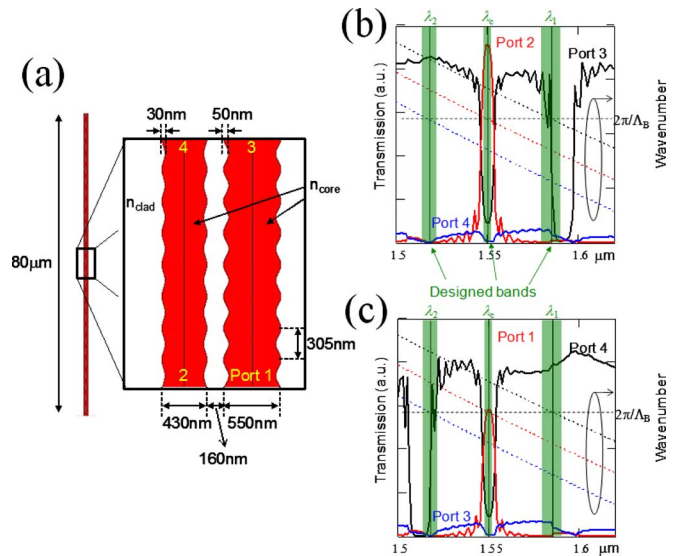


FIG. 2. (Color online) (a) Geometry of the designed device. [(b) and (c)] Spectra at the output ports calculated by 2D FDTD, when the incident light is introduced into Port1 and Port2, respectively.

$=\lambda^2|\kappa_i|/\pi n_{\text{eff}}$ and the corresponding Bragg lengths, $L_{B_i}=1/|\kappa_i|$, where $i=1, 2, c$, and n_{eff} is the effective index for WG1 or WG2 for the backward couplings, but the average effective index is used for the cross coupling. Figure 1(d) shows the plots of the bandwidth $\Delta\lambda_c$ and Bragg length L_{B_c} for cross coupling with relation to the gap G , for several grating modulation depths, (i) $\Delta W_1=50$ nm and $\Delta W_2=0$ nm, (ii) $\Delta W_1=0$ nm and $\Delta W_2=30$ nm, and (iii) $\Delta W_1=50$ nm and $\Delta W_2=30$ nm. We observe that a larger grating depth and a smaller gap give a wider bandwidth and a shorter Bragg length. Here, we take $\Delta W_1=50$ nm and $\Delta W_2=30$ nm. Since in our e-beam writing system, the writing field with enough high resolution and without stitching function is limited by around 100 $\mu\text{m}\times 100$ μm , we determine the length of WSC as $L_{B_c}=80$ μm for this example. Thus, we have $G=160$ nm and $\Delta\lambda_c=4.6$ nm from Fig. 1(d). We can reduce the bandwidth by increasing the gap or decreasing the modulation depth of the gratings. However, in both cases, a longer interaction length is required for the same extinction. Note that a higher extinction and suppressed sidelobes will require a longer grating length than Bragg length and apodization of the grating.⁴ However, we focus on demonstrating the coupling function as these advanced design are not in the scope of this paper.

We performed 2D finite difference time domain (FDTD) simulations (see Fig. 2) to validate the device structure designed above which is summarized in the schematic diagram of Fig. 2(a). Due to the limited accuracy of the analytic effective index method, we have adjusted the grating period to 305 nm to assure operation at 1.55 μm . Figures 2(b) and 2(c) show the calculated spectra in the output ports for light incident in Port1 and Port2, respectively, with the designed bands indicated by green area. We can see that, the backward couplings in WG1 and WG2, and cross coupling occur almost at the designed wavelengths with a small error due to inaccuracy of the analytic effective index method. We also note that, due to the sinusoidal-shaped grating assumed in the FDTD simulation, the coupling coefficients are slightly higher than that of the square-shaped grating in the analysis, as observed from the wider bandwidths and the higher ex-

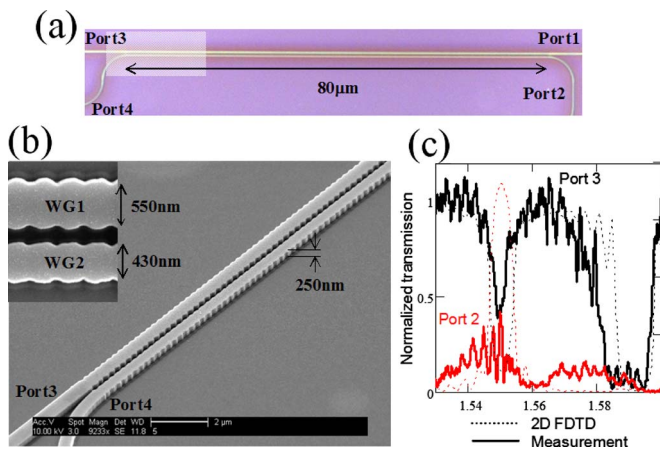


FIG. 3. (Color online) (a) Optical microscope image of the fabricated WSC device. (b) SEM micrograph of the area indicated by the shaded area in (a). (c) Measured transmission spectra with the input light introduced into Port1.

tion of the cross coupling than that for the Bragg length in the simulation results.

We fabricated the designed WSC on a silicon-on-insulator chip using e-beam lithography and reactive ion etching^{2,3} (see Fig. 3). Figure 3(a) shows the optical microscope image of the whole fabricated device whereas Fig. 3(b) shows the scanning electron microscope (SEM) micrograph of the magnified small area indicated in Fig. 3(a). We experimentally measured the transmission spectrum with the light incident on Port1 [see Fig. 3(c)]. The backward coupling in WG1 and the cross coupling occur at the desired wavelengths, whereas the extinction was less than those predicted by the simulation. We attribute the smaller extinction to the reduced coupling coefficient due to the incomplete uniformity (e.g., period fluctuation and sidewall roughness) and the incomplete dimensions of the gratings and the waveguides. The Fabry–Perot oscillation in the measured spectrum is found to be from the e-beam stitching error, according to the FSR of the oscillation. The small extinction can be increased by an improved fabrication and/or by a longer grating. Note that our device has very large FSR supporting the total bandwidth of about 70 nm used in WDM systems, whereas the FSR of a ring resonator implementation is limited to about 20 nm for typical ring designs with radius of about 5 μm .¹

Finally, we briefly discuss the applications of WSC. We could configure a multiport add-drop device by adding another VG waveguide and cascading the devices [see Fig. 4(a)]. When we add another VG waveguide with different waveguide width, as shown in the magnified view of Fig. 4(a), another cross coupling happens at a corresponding wavelength. Figure 4(b) shows the 2D FDTD simulation re-

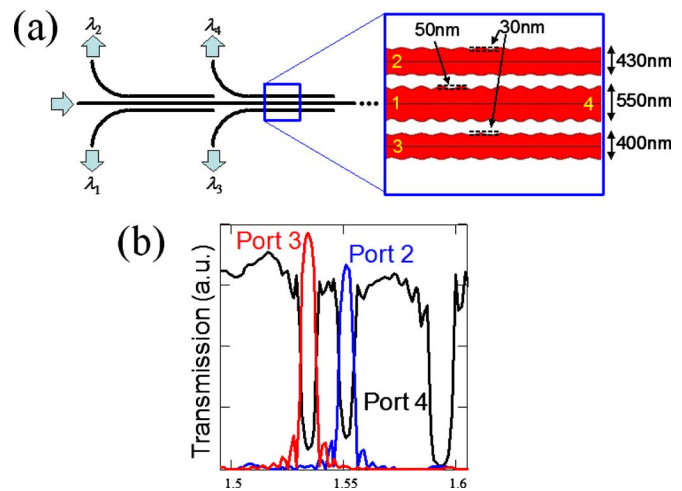


FIG. 4. (Color online) (a) Schematic diagram of multiport add-drop device with adding another waveguide and cascading the WSC. (b) 2D FDTD simulation results for the transmission spectrum to the output ports.

sult for the dimensions given in Fig. 4(a). We observe additional cross coupling at about 1.53 μm . The WSC structure can be also used in a ring resonator to select a single resonant mode from multiple resonant modes.

In conclusions, we introduced a WSC using VG structure on a silicon chip, and gave the operation principle and the analytic design procedure. The transmission spectra expected by the procedure agreed with FDTD simulation results. We fabricated the designed WSC and demonstrated the expected operation. The available WDM bandwidth of this device is not limited by FSR as in ring resonators.

The authors thank A. Krishnamoorthy and J. Cunningham at Sun Microsystems for valuable suggestions and encouragement and H.-C. Kim for developing the fabrication recipes and the measurement setups used in this work. Financial support from the National Science Foundation, the Air Force Office of Scientific Research, and the Defense Advanced Research Projects Agency are gratefully acknowledged. K. Ikeda acknowledges the scholarship from Nakajima Foundation, Japan.

¹V. R. Almeida, C. A. Barrios, R. R. Panepucci, and M. Lipson, *Nature (London)* **431**, 1081 (2004).

²H.-C. Kim, K. Ikeda, and Y. Fainman, *Opt. Lett.* **32**, 539 (2007).

³H.-C. Kim, K. Ikeda, and Y. Fainman, *J. Lightwave Technol.* **25**, 1147 (2007).

⁴J. T. Hastings, M. H. Lim, J. G. Goodberlet, and H. I. Smith, *J. Vac. Sci. Technol. B* **20**, 2753 (2002).

⁵P. Yeh and H. F. Taylor, *Appl. Opt.* **19**, 2848 (1980).

⁶A. Yariv and P. Yeh, *Optical Waves in Crystals* (Wiley, Hoboken, NJ, 2003).